ARTICLE

BODIPY and Dipyrrin as Unexpected Robust Anchoring Groups on TiO_2 Nanoparticles

Received 00th January 20xx,
Accepted 00th January 20xx

DOI: 10.1039/x0xx00000x

Josephine A. Jacob-Dolan,[a,b] Matt D. Capobianco,[a,b] Han-Yu Liu,[a,b] Cristina Decavoli,[a,b,c] Robert H. Crabtree,[a,b] and Gary W. Brudvig *[a,b]

Covalent attachment of molecules to metal oxide surfaces typically demands the presence of an anchoring group that in turn requires synthetic steps to introduce. BODIPY (4,4-difluoro-4-bora-3a,4a-diaza-*s*-indacene) chromophores have long been used in dye-sensitized solar cells, but carboxylic acid groups typically had to be installed to act as surface anchors. We now find that even without the introduction of such anchors, the unmodified BODIPY can bind to TiO_2 surfaces via its BF_2 group through boron–oxygen surface bonds. Dipyrrin, the parent molecule of BODIPY, is also capable of binding directly to TiO_2 surfaces, likely through its chelating nitrogen atoms. These binding modes, prove to be even more robust than that of an installed carboxylate and offer a new way to attach molecular complexes to surfaces for (photo)catalytic applications since, once bound, we show that surface bound BODIPY and dipyrrin derivatives exhibit ultrafast photoinjection of electrons into the conduction band of TiO_2.

Introduction

For the purpose of storing solar energy, there is interest in developing water-splitting devices powered by abundant solar photons.[1] One promising type of device is a water-splitting dye-sensitized photoelectrochemical cell (WS-DSPEC), in which two water molecules are converted into one oxygen molecule, four protons, and four electrons at the photoanode, and a fuel such as hydrogen is formed by proton reduction at the cathode.[2, 3] To build these photoanodes and photocathodes, molecular photosensitizers and catalysts must bind onto the surface of a wide-bandgap semiconductors such as TiO_2.[4-7] Current strategies for covalently attaching a dye to the semiconductor surface typically require the introduction of an anchoring group, such as a carboxylic or phosphonic acid, or a silatrane, all of which require careful design and additional synthetic efforts.[8-11] Here, we report a novel binding mode of BODIPY (4-difluoro-4-bora-3a,4a-diaza-s-indacene) chromophores onto TiO_2 without the need for any additional anchoring groups. This occurs through the boron as long as the 3 and 5 positions of the molecule (Figure 1a), typically methylated in most prior examples,[12, 13] are unsubstituted in order to avoid a steric clash with the surface.

BODIPY (Figure 1a) and its derivatives have long been used for biological imaging and optoelectronic applications due to their strong fluorescence.[14, 15] The molecule has also been used as a photosensitizer in dye-sensitized solar cells (DSSCs), though so far always attached through a specially introduced anchoring group. In many cases, the molecule is bound to the surface through a carboxylic group introduced into the para position of the 8-phenyl-BODIPY backbone (Figure 1b).[13, 16] In other instances, the 3, 5 positions of the pyrrole rings are functionalized with linkers and anchoring groups for surface

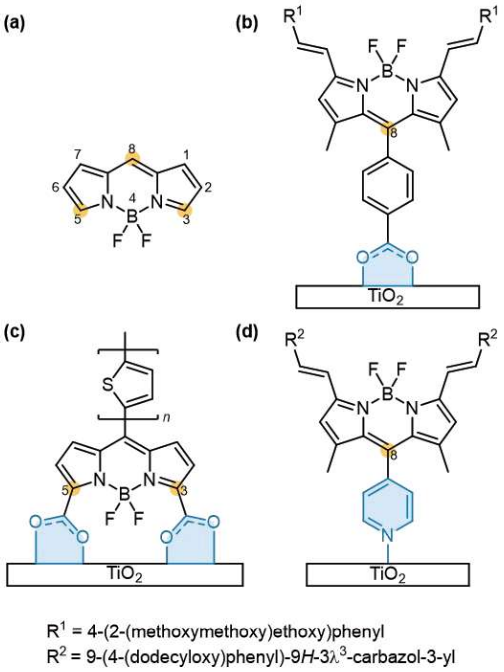

R^1 = 4-(2-(methoxymethoxy)ethoxy)phenyl
R^2 = 9-(4-(dodecyloxy)phenyl)-9*H*-3λ^3-carbazol-3-yl

Figure 1. (a) BODIPY backbone and IUPAC numbering system for BODIPY dyes, (b) example of surface binding on TiO_2 via a carboxylic acid at the 8 position,[16] (c) example of surface binding by substitutions at the 3, 5 positions,[17] (d) example of surface binding via a pyridine substitution at the 8 position[19].

---

[a] Department of Chemistry, Yale University, New Haven, Connecticut 06520-8107, USA.
[b] Energy Sciences Institute, Yale University, West Haven, Connecticut, 06516, USA
[c] Department of Materials Science and INSTM Unit, Solar Energy Research Center MIB-SOLAR, University of Milano – Bicocca, Milano, I-20125, Italy
*Corresponding author: gary.brudvig@yale.edu

Electronic Supplementary Information (ESI) available: details on materials and terahertz measurements, additional surface loading data, XPS, IR, and OPTP spectra. See DOI: 10.1039/x0xx00000x attachment (Figure 1c).[17] BODIPY has also been used in light-harvesting antenna systems on TiO_2 where a porphyrin is synthetically linked to a BODIPY and then loaded onto the metal oxide through a carboxylic acid linker on the porphyrin.[18] These methods have been successful and result in high surface coverage of metal oxide surfaces in DSSCs. However, in WS-DSPECs, carboxylic acid anchoring groups are problematic: they suffer from limited stability in aqueous systems, can be difficult to purify, and can bind to the metal center of any nearby catalyst. Other anchors have also been successful; for example, the Ishihara group used a pyridyl group attached at the 8-position to connect the BODIPY to TiO_2 on a photocathode for hydrogen production (Figure 1d).[19] This method is synthetically simpler than for the carboxylic acid case, and the anchor proved stable for over 120 hours. Even with these improvements, there is still a need to look for other, more robust binding modes.

Since the 3 and 5 positions of BODIPY are often substituted, it is no surprise that prior studies of surface attachment have involved these substituted BODIPYs. This substitution is typically preferred because it provides many benefits, including higher molar absorption coefficients,[20, 21] greater fluorescence quantum yields,[22] a red shift of the visible absorption,[12] and good synthetic and commercial availability.[12] However, the steric bulk of these substituents prevents the boron atom from having any direct interaction with the surface.

In addition to using BODIPY as a dye, a few groups have also utilized dipyrrin, the parent molecule of BODIPY lacking the BF_2 group, as a ligand for metal-centered photosensitizers.[23-25] However, we were not able to find any example in the literature of dipyrrin molecules binding directly to the surface of TiO_2 or any other metal oxide.

As an alternative to the synthetic introduction of anchoring groups to the BODIPY framework, we now report that 3,5-unsubstituted 8-phenyl-BODIPY (**2**) can bind to TiO_2 nanoparticles without any need for modification. The molecule contains its own anchoring group, the BF_2 unit, and, once bound, it can act as a molecular photosensitizer for TiO_2.

To better understand the loading of **2** onto TiO_2, we compared this molecule to three other compounds with the same 8-phenyl-dipyrrin backbone (Figure 2). We chose a 3,5-unsubstituted 8-phenyldipyrrin bromide salt (**1**) both as a model compound to compare with **2**, as well as to see if dipyrrin alone can function as an anchoring group. As has been reported before, we found that the salt was much more stable than the free base and therefore gave more reproducible results.[26] Molecules **3** and **4** were selected to see how substitutions of the 3 and 5 position affect loading onto TiO_2. For comparison with the standard carboxylate anchoring group, **4** was included in the loading and stability studies.

Experimental

Instrumentation

UV-visible absorption spectra were collected using a Shimadzu UV-2600 spectrophotometer. Solid-state absorption spectra of thin films were taken using the integrating sphere attachment. X-ray photoelectron spectroscopic measurements were performed using a PHI VersaProbe II Scanning XPS Microprobe. Attenuated total reflectance Fourier transform infrared (ATR-FTIR) spectroscopic measurements were performed using an Agilent Technologies Cary 600 Series FTIR spectrometer and a PIKE technologies GladiATR. ^1H, ^{11}B, ^{13}C, and ^{19}F NMR data were collected using an Agilent 400 MHz NMR instrument. A Bruker Dektak XT stylus profilometer was used to measure TiO_2 film thicknesses. All sonication procedures were carried out with a benchtop bath sonicator.

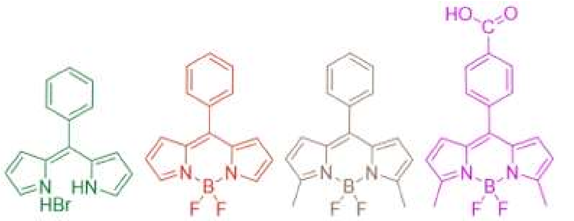

1 **2** **3** **4**

Figure 2. Structures of compounds used for our investigations.

Synthesis

(*Z*)-2-(phenyl(2*H*-pyrrol-2-ylidene)methyl)-1*H*-pyrrole hydrobromide (**1**),[26] (*T*-4)-difluoro[2-[phenyl(2*H*-pyrrol-2-ylidene-κ*N*)methyl]-1*H*-pyrrolato-κ*N*]boron (**2**),[27, 28] (*T*-4)-difluoro[2-methyl-5-[(5-methyl-2*H*-pyrrol-2-ylidene-κ*N*)phenylmethyl]-1*H*-pyrrolato-κ*N*]boron (**3**),[29] (*T*-4)-difluoro[4-[(5-methyl-1*H*-pyrrol-2-yl-κ*N*)(5-methyl-2*H*-pyrrol-2-ylidene-κ*N*)methyl]benzoic acid]boron (**4**),[30] and (*T*-4)-[1,2-benzenediolato(2-)-κ*O*^{1},κ*O*^{2}][2-[phenyl(2*H*-pyrrol-2-ylidene-κ*N*)methyl]-1*H*-pyrrolato-κ*N*]boron (**5**)[31] have been synthesized by literature procedures and the structures were confirmed by ^1H, ^{11}B, ^{13}C, and ^{19}F NMR.

Thin Film Preparation

Thin films of TiO_2 were formed on plain glass microscope slides except for the terahertz experiments which required quartz substrates. In both cases, the slides were first cleaned via sonication to remove any surface contamination that might be present. Each sonication step took about 15 minutes beginning with water and followed by acetone, isopropanol, and ethanol. After sonication, the slides were then blown dry with air. One layer of TiO_2 was deposited onto the clean substrate by using a doctor-blade method, using commercial TiO_2 paste and one layer of Scotch® Magic™ Tape as the barrier. Ti-Nanoxide T/SP paste was purchased from Solaronix and used as received. The samples were then thermally annealed in a box oven by heating from 25 to 370 °C at a rate of 180 °C/h, holding at 370 °C for 10 min, followed by heating to 480 °C at a rate of 180 °C/h, holding at 480 °C for 30 min, and finally returning to room temperature through ambient cooling. The resulting thickness of the films was ~4 µm as determined by profilometry.

Figure 3. (a) UV-visible spectra of **1–4** in acetonitrile solutions (b) UV-visible spectra of **1–4** loaded on TiO_2 with the absorbance of bare TiO_2 subtracted.

Procedure for Binding 1–4 to TiO_2 Thin Films

Thin TiO_2 films were loaded with molecules **1–4** (Figure 2), all following the same procedures. In each case, a 5 mM solution was made by dissolving the corresponding compound in dry acetonitrile. The TiO_2 films on glass were then dipped into the solution and soaked for 6 hours at room temperature in the dark. We found that anhydrous conditions greatly improve the loading of BODIPY onto the TiO_2 films. This was imperative for good reproducibility of the findings and could potentially explain why previous studies of BODIPY have not found this binding mode. We made sure to use dry solvents and oven-dried glassware and to store the TiO_2 films in the drying oven before use. Following the sensitization, the films were thoroughly rinsed with dry acetonitrile and dried in a stream of nitrogen.

Results and Discussion

Surface Loading

Through sensitization of TiO_2 films on glass with molecules **1–4**, we found that **1**, **2**, and **4** all showed significant loading on TiO_2 (Figure S1); however, compound **3** was found to have only minimal loading (Figure 3). The UV-visible spectra of the molecules in acetonitrile solution are shown in Figure 3a. As seen in previous studies, there is a significant increase in the molar absorptivity of compounds **3** and **4**, due to the methyl groups in the 3,5 positions of the BODIPY.[20, 21] Once these molecules were loaded onto TiO_2, the UV-visible absorbance was measured using an integrating sphere. Figure 3b shows a significant sloping baseline for **2**, and to a lesser extent for **1**, loaded on TiO_2 film, but this is not observed for **3** or **4**. We attribute this effect to an increased electronic coupling between the dye and the TiO_2, as previously observed for surface-bound catechol on TiO_2.[32-36] When the dye is progressively removed from the surface, the baseline decreases at the same rate as the peak associated with the absorption of **2** (Figure S2) indicating that the effect is associated with the presence of the dye and not some other effect. To calculate an appropriate loading number of **2**, we subtracted the sloping baseline and only report in Figure S3 the absorbance that can be attributed to the loaded dye itself. This will likely create an underestimation of the loading since the proposed orbital mixing will decrease the molar absorptivity at the λ_{max} of **2**.[37, 38] For consistency, we repeated this baseline-subtraction procedure for all four molecules, though the difference in the baseline was less significant in the other three cases, consistent with our hypothesis that **2** binds in a unique fashion to the surface. Using the adjusted absorbance, we then quantified the loading (Γ) using Equation (1), where A is the absorbance of the loaded film at specified wavelength λ, ε is the molar absorptivity at the same wavelength λ, and ℓ is the thickness of the film as measured by mechanical profilometry.[39]

$$\Gamma(\text{mol cm}^{-2}\,\mu\text{m}^{-1}) = A(\lambda) / (1000\,\varepsilon \cdot \ell) \qquad (1)$$

From this analysis, we found the loading of **2** to be (1.6 ± 0.1) × 10^9 mol cm^{-2} μm^{-1} (Table S1). This is about 60% of the loading seen for **4** but, as mentioned above, is most likely an underestimation.

Binding Mode Determination

After establishing that these molecules loaded onto TiO_2, we wanted to know how **2** is binding to the surface. Our hypothesized binding modes can be seen in Figure 4. Based on the UV-visible spectra in Figure 3, we propose that **1** binds by chelating to a titanium atom with the pyrrolic nitrogen atoms. This is supported by a shift in the UV-visible spectrum to longer

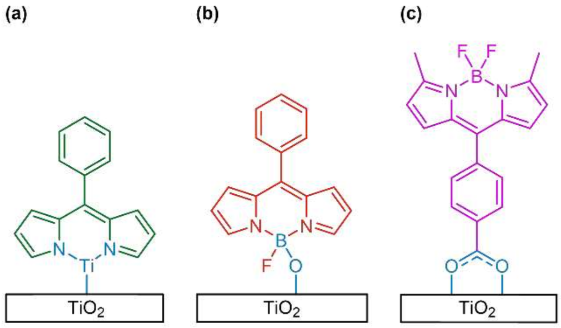

Figure 4. Hypothesized binding modes for **1**/TiO_2, **2**/TiO_2 and **4**/TiO_2.

wavelengths upon loading which is similar to the shift observed when dipyrrin is metalated in the molecular form.[40] We determined that **2** retains the BF_2 group and does not bind in the dipyrrin form (**1**) on the surface. If loss of the BF_2 group were occurring, we would not expect to see any difference between the spectra of the bound **1**/TiO_2 and the bound **2**/TiO_2, but we instead observe that in both cases the spectra retain a similar shape to the solution species and notice only the previously discussed sloping baselines. The data suggest that the methyl groups in the 3 and 5 positions of the dipyrrole hinder the binding of **3** to the surface implying that the boron and surface must be able to interact for loading to occur, and steric hindrance can prevent this from happening. In the case of **4**, we are able to attribute nearly all of the loading to the carboxylic acid group, assuming that, as is the case with **3**, the methyl groups will block binding through the boron.

X-ray photoelectron spectroscopy (XPS) gave further evidence that the boron in **2** is still bound to the dipyrrin when loaded onto TiO_2, as shown in Figure 5. Boron can be difficult to resolve by XPS but by using a high scan number and high power, we were able to resolve the boron peak for **2** and **4** both in their free forms well as loaded onto TiO_2 films. For comparison, the baselines from bare TiO_2 and **1**-loaded films can be seen in Figure S4a. To better resolve the peaks, a Savitzky–Golay smoothing procedure was used.[41] In addition to confirming the presence of boron on the loaded films, we also compared the binding energies of the boron in the molecules alone to that of the molecules loaded on TiO_2. In Figure 5, it is clear that there is a shift to lower binding energy for the boron in **2** when loaded onto TiO_2. A lower binding energy implies a greater electron density around boron, suggesting a change in the coordination environment of the boron. This is consistent with the hypothesis that a less electron withdrawing ligand, O, has replaced one or both of the fluorides. We suggest that a surface hydroxyl has attacked the boron and after displacing a fluoride ion has formed a boron–oxygen bond to the surface. To test this hypothesis, we synthesized **5** (Figure 5) as a surface model, where the boron is bound to the same dipyrrin ligand as **2**, but the fluorides are substituted for oxygens. The binding energy of the boron in **5** is shifted to the same energy as for **2** bound to TiO_2, consistent with our proposal that **2** covalently binds to the TiO_2 surface via B–O bonds. In the case of dye **4**, there is no shift in the binding energy of boron when loaded onto TiO_2, which is consistent with the molecule binding through the carboxylic acid with no change to the boron coordination. Since TiO_2 surfaces have a high affinity for binding fluoride,[42, 43] displaced fluorides from **2** could bind in this way. When looking at the fluorine XPS, we noticed signal broadening for **2** loaded onto TiO_2 which was not evident in **4** (Figure S4b). This is consistent with one fluoride remaining on the boron and one departing and binding to the TiO_2; however, due to the presence of fluoride in the bare commercial TiO_2 nanoparticles, this hypothesis needs to be tested with additional experiments.

IR data further corroborated our hypothesis of the binding mode of these compounds onto TiO_2, though it was difficult to resolve the stretches of **2** bound to TiO_2. Figure 6 compares free **1**, **2** and **4** with the molecules loaded on TiO_2 films. It is interesting to notice that well resolved peaks are visible for **1**/TiO_2 and **4**/TiO_2, but the peaks are very broad in **2**/TiO_2. The broadening of the IR stretches in **2**/TiO_2 could be due to the

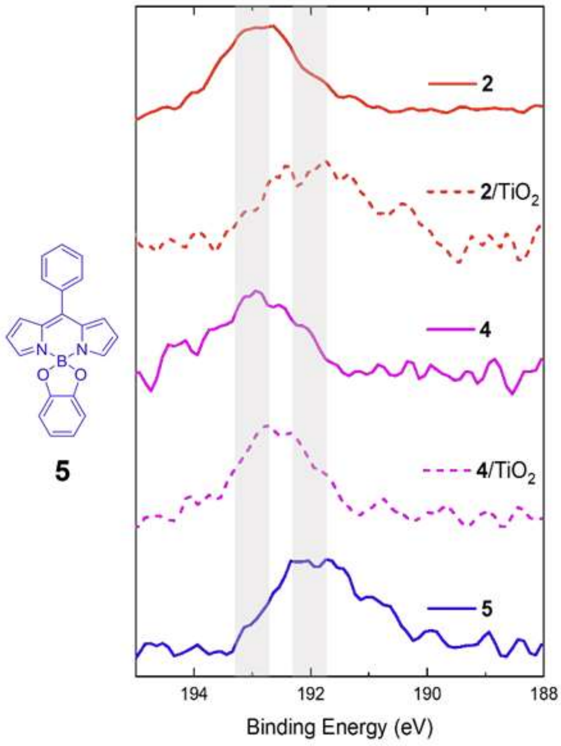

Figure 5. XPS data showing the binding energy of the boron atom in powder samples of molecular **2**, **4**, and **5** as well as **2** and **4** loaded on TiO_2. The grey bars are meant to help guide the eye.

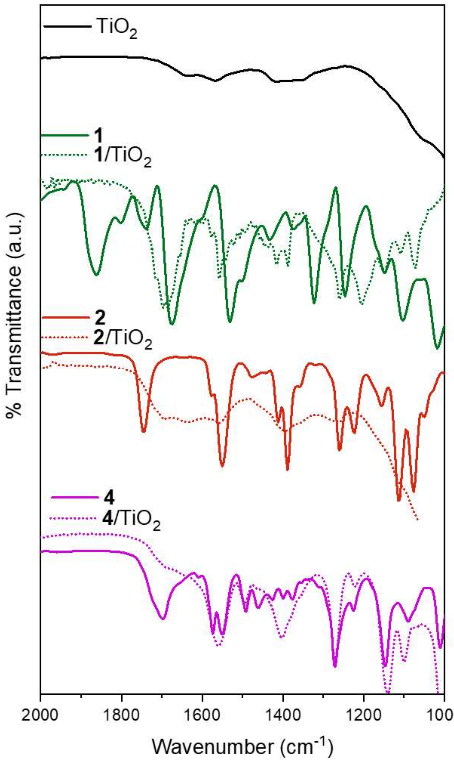

Figure 6. FTIR spectra comparing **1**, **2**, and **4** as powder samples and loaded onto TiO_2 films.

occurrence of a variety of binding modes on the surface. We assigned the following as B–F stretches of **2**: 1110 cm^{-1} (asymmetric) and 1076 cm^{-1} (symmetric)[31] and of **4**: 1145 cm^{-1} (asymmetric) and 1093 cm^{-1} (symmetric). We attribute the difference in amplitude between the asymmetric and symmetric stretches in the case of **4** to the steric effects of the methyl groups in the 3 and 5 positions. The same pattern is seen for **3** where the methyl groups are similarly substituted on the pyrrole (Figure S6). When comparing the free molecules to the ones loaded on TiO_2 it is clear that the B–F stretch in **4** remains unchanged while the C=O stretch at 1720 cm^{-1} does significantly weaken. This is expected if **4** binds through the carboxylic acid group and no change occurs to the BF_2 group. In **2,** it is more difficult to resolve the peaks of the loaded film; however, there is no sign of a B–F stretch near 1064 cm^{-1} after loading onto TiO_2. This suggests that the TiO_2 surface oxygens could be displacing the fluorides of **2**. We attempted to probe the proposed resulting B–O bond in **2** on TiO_2 by Raman spectroscopy; however, the strong fluorescence of **2** does not allow for any features to be resolved, even when using an excitation wavelength of 780 nm.

Stability of Binding

We next compared the stability of binding of **1**, **2** and **4** on TiO_2. We were interested in the stability in water for applications in WS-DSPECs as well as in acetonitrile, as this is the solvent we used for sensitization and offers high solubility for the series of compounds. **2** remains 60% loaded on the surface when soaked in water for 24 hours as is seen in Figure 7 but this may be attributed in part to the insolubility of **2** in water. However, **2** also remains 70% loaded on the surface when soaked in dry acetonitrile for 24 hours, a solvent in which it is very soluble. **2** was quickly removed when soaked in a mixed solvent consisting of water and acetonitrile in a 1:1 ratio, suggesting that water may be able to hydrolyze the BODIPY–surface bonds with a suitable cosolvent present. We find two distinct desorption regimes in acetonitrile and in water. A fast desorption at early times is followed by much slower desorption at later times. This suggests that there are two different surface attachment modes at play, with one being much weaker than the other.[44, 45] Once the weakly attached species are removed in the first few hours, the more strongly bound species remain bound over the course of the experiment.

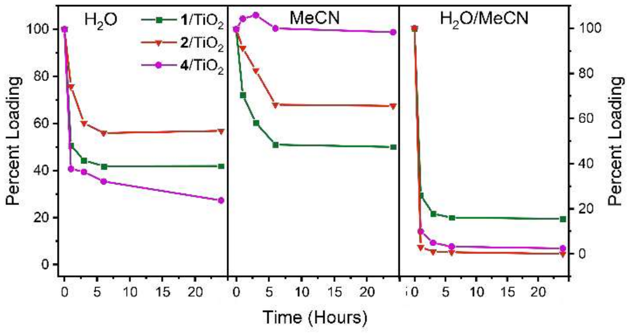

Figure 7. Stability of **1**, **2**, and **4** on TiO_2 in water, acetonitrile, and a 1:1 (v/v) water–acetonitrile mixture.

As has been observed in stability studies of dyes anchored on TiO_2 via carboxylic acids, surface-attached **4** was somewhat labile in neutral water, retaining only 30% of the loaded dye after 24 hours (Figure 7);[46] however, in dry acetonitrile, **4** was very stable with >95% still loaded after 24 hours. **1** and **2** had similar stabilities and desorption dynamics in water and acetonitrile. All three molecules were nearly completely removed within an hour with a water-acetonitrile mixed solvent.

Charge Injection

We next wanted to see if the surface-bound **2** could also act as a photosensitizer, and how it compares to **1** and **4**. Optical pump terahertz probe (OPTP) spectroscopy is a common way to probe electron injection from a photosensitizer into the conduction band of the semiconductor.[39, 47] Since terahertz radiation is sensitive to mobile electrons, any attenuation in terahertz transmission can be attributed to the injection of electrons into the conduction band of the semiconductor.[48] Figure 8 displays the OPTP data for **1**, **2**, and **4** anchored on TiO_2, confirming ultrafast charge injection. This is convincing evidence that the anchoring chemistry does not inhibit the BODIPY derivatives from functioning as photosensitizers as would be needed in a DSSC or WS-PEC. The same measurement was also repeated for **1** and **4** loaded on TiO_2 with similar results. There is a difference in the ΔTHz (Figure 8) and in the recombination and/or trapping kinetics for **1** and **4** versus **2** as shown by normalized OPTP traces (Figure S7). This implies that there are different injection mechanisms into the metal oxide, but further spectroscopic studies are required to learn more.

Conclusions

The covalent binding of **1** and **2** to TiO_2 nanoparticles is unexpected and provides new anchoring groups. We found that dipyrrin and BODIPY derivatives are able to bind directly onto TiO_2 nanoparticles through the boron atom, as long as the 3 and 5 positions of the pyrrole are unsubstituted. The surface-bound molecule retains the boron atom and likely binds after loss of a fluoride to form a boron–oxygen bond to the surface. We also found that molecule **2** loaded in this way exhibits ultrafast electron injection into the conduction band of TiO_2 nanoparticles, indicating the electron injection is not inhibited

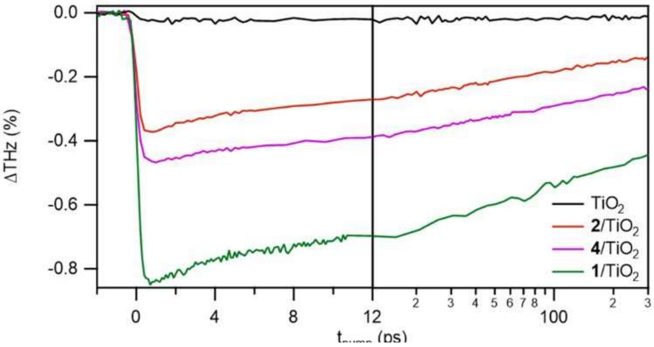

Figure 8. OPTP trace of **1**, **2**, and **4** loaded onto TiO_2 showing that all three dyes are capable of ultrafast injection of electrons into the conduction band of TiO_2.

by any binding-induced structural changes. This binding strategy offers a high extent of loading and persistent adhesion in water, making BODIPY derivatives potentially useful molecules for further applications in WS-PEC devices, a topic we are currently testing.

Author Contributions

The manuscript was written through contributions of all authors. All authors have given approval to the final version of the manuscript.

Conflicts of interest

There are no conflicts to declare.

Acknowledgements

We thank the staff at the Yale West Campus Analytical Core and Materials Characterization Core for their help with the instrumentation. This work was supported by the U.S. Department of Energy, Chemical Sciences, Geosciences, and Biosciences Division, Office of Basic Energy Sciences, Office of Science (Grant DE-FG02-07ER15909). Additional support was provided by a generous donation from the TomKat Charitable Trust.

References

1. K. J. Young, L. A. Martini, R. L. Milot, R. C. Snoeberger, V. S. Batista, C. A. Schmuttenmaer, R. H. Crabtree and G. W. Brudvig, *Coord. Chem. Rev.*, 2012, 256, 2503-2520.
2. M. K. Brennaman, R. J. Dillon, L. Alibabaei, M. K. Gish, C. J. Dares, D. L. Ashford, R. L. House, G. J. Meyer, J. M. Papanikolas and T. J. Meyer, *J. Am. Chem. Soc.*, 2016, 138, 13085-13102.
3. M. G. Walter, E. L. Warren, J. R. McKone, S. W. Boettcher, Q. Mi, E. A. Santori and N. S. Lewis, *Chem. Rev.*, 2010, 110, 6446-6473.
4. Z. Yu, F. Li and L. Sun, *Energy Environ. Sci.*, 2015, 8, 760-775.
5. F. Niu, D. Wang, F. Li, Y. Liu, S. Shen and T. J. Meyer, *Advanced Energy Materials*, 2020, 10, 1900399.
6. J. R. Swierk and T. E. Mallouk, *Chem. Soc. Rev.*, 2013, 42, 2357-2387.
7. C. Decavoli, C. L. Boldrini, N. Manfredi and A. Abbotto, *Eur. J. Inorg. Chem.*, 2020, 2020, 978-999.
8. K. L. Materna, R. H. Crabtree and G. W. Brudvig, *Chem. Soc. Rev.*, 2017, 46, 6099-6110.
9. H.-Y. Liu, C. C. Cody, J. A. Jacob-Dolan, R. H. Crabtree and G. W. Brudvig, *ACS Energy Lett.*, 2020, 5, 3195-3202.
10. J. L. Troiano, R. H. Crabtree and G. W. Brudvig, *ACS Appl Mater Interfaces*, 2022, 14, 6582-6589.
11. L. Zhang and J. M. Cole, *ACS Appl Mater Interfaces*, 2015, 7, 3427-3455.
12. A. Loudet and K. Burgess, *Chem. Rev.*, 2007, 107, 4891-4932.
13. H. Klfout, A. Stewart, M. Elkhalifa and H. He, *ACS Appl Mater Interfaces*, 2017, 9, 39873-39889.
14. W. Zhang, A. Ahmed, H. Cong, S. Wang, Y. Shen and B. Yu, *Dyes Pigm.*, 2021, 185, 108937.
15. M. Poddar and R. Misra, *Coord. Chem. Rev.*, 2020, 421, 213462.
16. I. Gonzalez-Valls, A. Mirloup, T. Le Bahers, N. Keller, T. Cottineau, P. Sautet and V. Keller, *RSC Advances*, 2016, 6, 91529-91540.
17. J. Songkhao, R. Banerjee, S. Debnath, S. Narasimhan, N. Wannaprom, P. Vanalabhpatana, N. Seriani, R. Gebauer and P. Thamyongkit, *Dyes Pigm.*, 2017, 142, 558-571.
18. C. Y. Lee and J. T. Hupp, *Langmuir*, 2010, 26, 3760-3765.
19. X.-F. Shen, M. Watanabe, A. Takagaki, J. T. Song and T. Ishihara, *Catalysts*, 2020, 10, 535.
20. R. Gubaidullin, D. Nedopekina, A. Tukhbatullin, E. Davletshin and A. Spivak, *Chem. Proc.*, 2020, 3, 11.
21. G. M. Chu, I. Fernández, A. Guerrero-Martínez, C. Ramírez De Arellano and M. A. Sierra, *Eur. J. Inorg. Chem.*, 2016, 2016, 844-852.
22. K. Zlatić, H. B. E. Ayouchia, H. Anane, B. Mihaljević, N. Basarić and T. Rohand, *J. Photochem. Photobiol. A: Chem.*, 2020, 388, 112206.
23. G. Li, K. Hu, C. Yi, K. L. Knappenberger, G. J. Meyer, S. I. Gorelsky and M. Shatruk, *J. Phys. Chem. C*, 2013, 117, 17399-17411.
24. M. Weston, T. J. Reade, K. Handrup, N. R. Champness and J. N. O'Shea, *J. Phys. Chem. C*, 2012, 116, 18184-18192.
25. J. D. Hall, T. M. McLean, S. J. Smalley, M. R. Waterland and S. G. Telfer, *DTr*, 2010, 39, 437-445.
26. C. D. Smith and A. Thompson, *RSC Advances*, 2020, 10, 24273-24279.
27. J. K. Laha, S. Dhanalekshmi, M. Taniguchi, A. Ambroise and J. S. Lindsey, *Org. Process Res. Dev.*, 2003, 7, 799-812.
28. D. Prasannan, D. Raghav, S. Sujatha, H. Hareendrakrishna kumar, K. Rathinasamy and C. Arunkumar, *RSC Advances*, 2016, 6, 80808-80824.
29. W. Qin, M. Baruah, M. Van der Auweraer, F. C. De Schryver and N. Boens, *J. Phys. Chem. A*, 2005, 109, 7371-7384.
30. S. Kolemen, O. A. Bozdemir, Y. Cakmak, G. Barin, S. Erten-Ela, M. Marszalek, J.-H. Yum, S. M. Zakeeruddin, M. K. Nazeeruddin, M. Grätzel and E. U. Akkaya, *Chem Sci*, 2011, 2, 949-954.
31. V. J. Richards, A. L. Gower, J. E. H. B. Smith, E. S. Davies, D. Lahaye, A. G. Slater, W. Lewis, A. J. Blake, N. R. Champness and D. L. Kays, *Chem. Commun.*, 2012, 48, 1751.
32. T. Lana-Villarreal, A. Rodes, J. M. Pérez and R. Gómez, *J. Am. Chem. Soc.*, 2005, 127, 12601-12611.
33. D. Finkelstein-Shapiro, S. K. Davidowski, P. B. Lee, C. Guo, G. P. Holland, T. Rajh, K. A. Gray, J. L. Yarger and M. Calatayud, *J. Phys. Chem. C*, 2016, 120, 23625-23630.
34. W. R. McNamara, R. C. Snoeberger, G. Li, J. M. Schleicher, C. W. Cady, M. Poyatos, C. A. Schmuttenmaer, R. H. Crabtree, G. W. Brudvig and V. S. Batista, *J. Am. Chem. Soc.*, 2008, 130, 14329-14338.
35. I. A. Janković, Z. V. Šaponjić, E. S. Džunuzović and J. M. Nedeljković, *Nanoscale Res. Lett.*, 2009, 5, 81.
36. P. A. Connor, K. D. Dobson and A. J. McQuillan, *Langmuir*, 1995, 11, 4193-4195.
37. G. Orlandi and W. Siebrand, *J. Chem. Phys.*, 1973, 58, 4513-4523.

38. M. Irikura, Y. Tamaki and O. Ishitani, *Chem. Sci.*, 2021, 12, 13888-13896.
39. J. Jiang, J. A. Spies, J. R. Swierk, A. J. Matula, K. P. Regan, N. Romano, B. J. Brennan, R. H. Crabtree, V. S. Batista, C. A. Schmuttenmaer and G. W. Brudvig, *J. Phys. Chem. C*, 2018, 122, 13529-13539.
40. L. Yu, K. Muthukumaran, I. V. Sazanovich, C. Kirmaier, E. Hindin, J. R. Diers, P. D. Boyle, D. F. Bocian, D. Holten and J. S. Lindsey, *Inorg. Chem.*, 2003, 42, 6629-6647.
41. A. Savitzky and M. J. E. Golay, *Anal. Chem.*, 1964, 36, 1627-1639.
42. M. Samadpour, P. P. Boix, S. Giménez, A. Iraji Zad, N. Taghavinia, I. Mora-Seró and J. Bisquert, *J. Phys. Chem. C*, 2011, 115, 14400-14407.
43. M. V. Dozzi, C. D’Andrea, B. Ohtani, G. Valentini and E. Selli, *J. Phys. Chem. C*, 2013, 117, 25586-25595.
44. B. J. Brennan, C. Koenigsmann, K. L. Materna, P. M. Kim, M. Koepf, R. H. Crabtree, C. A. Schmuttenmaer and G. W. Brudvig, *J. Phys. Chem. C*, 2016, 120, 12495-12502.
45. C. Koenigsmann, T. S. Ripolles, B. J. Brennan, C. F. A. Negre, M. Koepf, A. C. Durrell, R. L. Milot, J. A. Torre, R. H. Crabtree, V. S. Batista, G. W. Brudvig, J. Bisquert and C. A. Schmuttenmaer, *Phys. Chem. Chem. Phys.*, 2014, 16, 16629-16641.
46. W. R. McNamara, R. L. Milot, H.-e. Song, R. C. Snoeberger Iii, V. S. Batista, C. A. Schmuttenmaer, G. W. Brudvig and R. H. Crabtree, *Energy Environ. Sci.*, 2010, 3, 917-923.
47. J. Neu, S. Ostresh, K. P. Regan, J. A. Spies and C. A. Schmuttenmaer, *J. Phys. Chem. C*, 2020, 124, 3482-3488.
48. S. H. Lee, K. P. Regan, S. Hedström, A. J. Matula, S. Chaudhuri, R. H. Crabtree, V. S. Batista, C. A. Schmuttenmaer and G. W. Brudvig, *J. Phys. Chem. C*, 2017, 121, 22690-22699.